Title

Partial Amelioration of Peripheral and Central Symptoms of Huntington's Disease via Modulation of Lipid Metabolism.

Journal

Journal of Huntington's disease, 5(1)

ISSN

1879-6397

Authors

Chen, Jane Y
Tran, Conny
Hwang, Lin
et al.

Publication Date

2016

DOI

10.3233/jhd-150181

Peer reviewed

HHS Public Access

Author manuscript

J Huntingtons Dis. Author manuscript; available in PMC 2016 August 29.

Published in final edited form as:

J Huntingtons Dis. 2016 ; 5(1): 65–81. doi:10.3233/JHD-150181.

Partial Amelioration of Peripheral and Central Symptoms of Huntington's Disease *via* Modulation of Lipid Metabolism

Jane Y. Chen[1], **Conny Tran**[1], **Lin Hwang**[2], **Gang Deng**[3], **Michael E. Jung**[3], **Kym F. Faull**[2,4], **Michael S. Levine**[1,4], and **Carlos Cepeda**[1]

[1]Intellectual and Developmental Disabilities Research Center, Semel Institute for Neuroscience and Human Behavior, David Geffen School of Medicine, University of California Los Angeles

[2]Pasarow Mass Spectrometry Laboratory, David Geffen School of Medicine, University of California Los Angeles

[3]Department of Chemistry and Biochemistry, David Geffen School of Medicine, University of California Los Angeles

[4]Brain Research Institute, David Geffen School of Medicine, University of California Los Angeles

Abstract

Background—Huntington's disease (HD) is a fatal, inherited neurodegenerative disorder characterized by uncontrollable dance-like movements, as well as cognitive deficits and mood changes. A feature of HD is a metabolic disturbance that precedes neurological symptoms. In addition, brain cholesterol synthesis is significantly reduced, which could hamper synaptic transmission.

Objective—Alterations in lipid metabolism as a potential target for therapeutic intervention in the R6/2 mouse model of HD were examined.

Methods—Electrophysiological recordings *in vitro* examined the acute effects of cholesterol-modifying drugs. In addition, behavioral testing, effects on synaptic activity, and measurements of circulating and brain tissue concentrations of cholesterol and the ketone β-hydroxybutyrate (BHB), were examined in symptomatic R6/2 mice and littermate controls raised on normal chow or a ketogenic diet (KD).

Results—Whole-cell voltage clamp recordings of striatal medium-sized spiny neurons (MSNs) from symptomatic R6/2 mice showed increased frequency of spontaneous inhibitory postsynaptic currents (sIPSCs) compared with littermate controls. Incubation of slices in cholesterol reduced the frequency of large-amplitude sIPSCs. Addition of BHB or the Liver X Receptor (LXR) agonist T0901317 reduced the frequency and amplitude of sIPSCs. Surprisingly, incubation in simvastatin to reduce cholesterol levels also decreased the frequency of sIPSCs. HD mice fed the KD lost weight more gradually, performed better in an open field, had fewer stereotypies and lower brain levels of cholesterol than mice fed a regular diet.

Address for Correspondence: Carlos Cepeda, PhD, IDDRC, Semel Institute for Neuroscience, Room 58-258, UCLA School of Medicine, 760 Westwood Plaza, Los Angeles, CA 90024, Tel: (310) 206-0861, Fax: (310) 206-5060, ccepeda@mednet.ucla.edu.

Conflict of Interest

The authors declare they have no conflict of interest to report.

Conclusions—Lipid metabolism represents a potential target for therapeutic intervention in HD. Modifying cholesterol or ketone levels acutely in the brain can partially rescue synaptic alterations, and the KD can prevent weight loss and improve some behavioral abnormalities.

Keywords

R6/2 model; cholesterol; ketogenic diet; electrophysiology; synaptic activity

Introduction

The neuropathological hallmark of Huntington's disease (HD) is the degeneration of striatal medium-sized spiny neurons (MSNs) [1]. However, cell loss also has been observed in other brain regions such as the cerebral cortex, thalamus, and hypothalamus [2–4]. HD studies are increasingly focusing on metabolic disturbances. Loss of orexin neurons in the hypothalamus of HD patients leads to metabolic imbalance [3] and elevated caloric intake occurs in individuals at risk of developing HD [5]. Clinical studies have demonstrated deficits in insulin secretion capacity and a simultaneous decrease in insulin sensitivity in normoglycemic patients with HD compared with controls [6]. In addition to balancing free glucose and stored glycogen, insulin regulates triglyceride production and fatty acid synthesis [7]. Similar to HD patients, genetic mouse models of HD display impaired glucose metabolism [8, 9], alterations in adipose tissue [10], as well as insulin and leptin resistance [11]. Deficient glucose metabolism necessitates alternative sources to satisfy energetic demands. One potential candidate is lipid metabolism, in particular ketone bodies [12, 13].

In HD patients and mouse models of HD, growing evidence has demonstrated early and long-lasting alterations in the cholesterol biosynthetic pathway [14]. The principal function of cholesterol is to maintain the integrity of cell membranes and in the brain, it is essential for myelin formation, membrane fluidity, neurosteroid production, and synaptic activity [15]. When cholesterol is reduced, spontaneous glutamate synaptic neurotransmission increases whereas evoked responses decrease [16]. In addition, cholesterol is an essential component of lipid rafts, specialized membrane microdomains that regulate neurotransmission, receptor trafficking, synapse maintenance, and spine density [17]. Importantly, lipid rafts display early alterations in mouse models of HD [18].

Brain cholesterol is synthesized locally from acetyl-CoA and requires complex machinery to maintain steady-state levels [19]. Brain-generated cholesterol does not cross the blood-brain barrier (BBB), but 24-OHC, an oxygenated metabolite of cholesterol, is capable of diffusing into the bloodstream [20]. Mutant huntingtin (mHtt) inhibits the transcription of sterol regulatory element (SRE)-regulated gene products that are essential for cholesterol biosynthesis [14]. Changes in brain cholesterol synthesis and levels are particularly evident in HD mouse models [14, 21, 22] and *in vitro* addition of exogenous cholesterol to striatal neurons expressing mHtt prevents cell death [22]. Thus, restoring normal cholesterol levels can be neuroprotective.

A wide array of intrinsic and synaptic membrane properties are altered in HD genetic mouse models [23]. MSNs and cortical pyramidal neurons display a depolarized resting membrane potential, probably as a consequence of reduced energy substrates [24–26]. In addition, in

different mouse models of HD we demonstrated early and progressive alterations in glutamatergic transmission along the corticostriatal pathway [24, 27]. GABA synaptic activity also is altered. A significant increase in the frequency of spontaneous inhibitory postsynaptic currents (sIPSCs) occurs in a subpopulation of MSNs. This finding led us to suggest that increased inhibition dampens striatal output and can explain some of the behavioral symptoms [28, 29]. Thus, reducing intrastriatal GABA transmission can be a potential therapeutic target.

In the present study we combined *in vitro* and *in vivo* experiments to examine the potentially ameliorative effects of manipulations of lipid metabolism, in particular the cholesterol pathway, in the transgenic R6/2 mouse model of HD. We chose this model because it has become a standard for drug testing [30] and has been well-characterized both behaviorally and electrophysiologically in our laboratory. If, as evidence suggests, cholesterol synthesis and levels are reduced in HD [14, 31], cholesterol supplementation could be beneficial. In particular, based on the observation that cholesterol depletion leads to an increase in spontaneous neurotransmitter release [16], we hypothesized that by increasing cholesterol we could reduce the increase in sIPSC frequency observed in HD models [29]. To test this hypothesis, we incubated striatal slices in a number of compounds known to modulate cholesterol synthesis and levels. For cholesterol supplementation we used cholesterol itself. To provide another energy substrate in mice with deficient glucose metabolism, β-hydroxybutyrate (BHB), a ketone body was used [32]. We also tested the effects of T0901317, a liver X receptor (LXR) agonist. LXRs are nuclear sensors that maintain cholesterol homeostasis so that when the concentration of cholesterol increases, LXRs induce transcription of genes that protect cells from cholesterol overload [33]. Finally, to reduce cholesterol levels we used simvastatin, an inhibitor of 3-hydroxy-3-methyl-glutaryl-CoA (HMG-CoA) reductase, the enzyme necessary for the production of endogenous cholesterol. After acute incubation of these compounds we examined *in vitro* membrane and synaptic properties of MSNs in symptomatic HD mice and littermate controls. We also examined the chronic effects of a ketogenic diet (KD) on behavioral alterations and MSN electrophysiology. The KD has been proved beneficial in epilepsy [34, 35] and Alzheimer's disease [36]. Further, the KD increases the production of BHB [37] and while cholesterol and fatty acids do not appear to cross the BBB, ketones can enter the brain and serve as energy substrates [37]. We demonstrate that increasing cholesterol and ketone levels in the brain, or stimulating cholesterol efflux, can rescue some altered synaptic properties and animals fed a KD show delayed weight loss and improvement in behavioral deficits.

Methods

Animals

All procedures were performed in accordance with the U.S. Public Health Service Guide for Care and Use of Laboratory Animals and were approved by the Institutional Animal Care and Use Committee at the University of California Los Angeles. Mice were obtained from our R6/2 breeding colony. This colony is maintained by breeders (line 2801) from the Jackson Laboratory (Bar Harbor, ME). R6/2 mice were bred by crossing WT C57BL6xCBA-F1 males with WT C57BL6xCBA females containing ovaries transplanted

from hemizygous R6/2 mice. Experimental mice were housed on a 12h light-dark cycle with lights on from 7:00–19:00. Food and water were available *ad libitum*. Genotyping was performed using PCR of DNA obtained from tail samples, once at weaning and again following the completion of behavioral testing and/or electrophysiological experiments to confirm the genotype. CAG repeat lengths for R6/2 mice were determined by Laragen Inc. (Culver City, CA) and found to be 153±1 (mean ± SE, n=23).

Electrophysiology

Mice were deeply anesthetized and intracardially perfused with 10 ml of ice-cold high-sucrose artificial cerebrospinal fluid (slice ACSF) containing (in mM): 26 $NaHCO_3$, 1.25 NaH_2PO_4, 2.5 KCl, 1.3 $MgCl_2$, 8 $MgSO_4$, 208 sucrose, and 10 glucose. They were then decapitated and the brains rapidly removed and placed in the same high-sucrose solution. Coronal slices (300 μm) were cut and incubated in regular ACSF containing 130 NaCl, 26 $NaHCO_3$, 1.25 NaH_2PO_4, 3 KCl, 2 $MgCl_2$, 2 $CaCl_2$, and 10 glucose (pH 7.2–7.35, 290–310 mOsm) and oxygenated with 95% O_2 – 5% CO_2. Slices were allowed to recover at room temperature for at least 1h before recordings. In some experiments we examined the effects of enriched ACSF (eACSF) on spontaneous synaptic activity in brain slices from control and symptomatic HD mice (~11 week-old). eACSF was made by addition of BHB, the main ketone body [12], and pyruvate to regular ACSF as follows (in mM): 130 NaCl, 26 $NaHCO_3$, 1.25 NaH_2PO_4, 3 KCl, 2 $MgCl_2$, 2 $CaCl_2$, 5 glucose, 5 pyruvate, 2 β-hydroxybutyrate (pH 7.2–7.35, Osmolarity 290–310 mOsm) [32]. First, slices were incubated and MSNs recorded in regular ACSF. After obtaining baseline data, the ACSF solution was replaced with eACSF for 20–30 min and the effects on synaptic activity were examined.

For cholesterol supplementation, slices were incubated for 1–2 h in a water-soluble formulation of cholesterol (10 μM, Sigma-Aldrich) pre-complexed with methyl-β-cyclodextrin (MCD) which serves as a carrier. To examine the effects of LXR activation a synthetic agonist, T0901317 (10 μM, Tocris) was used. To lower cholesterol levels simvastatin (10 μM, Tocris), an inhibitor of cholesterol synthesis [16], was used. After incubation, slices were transferred to the recording chamber and perfused with the same drug used during incubation. Except for cholesterol, all drugs were dissolved in DMSO (0.1%). At this concentration, DMSO by itself did not affect spontaneous synaptic activity.

Whole-cell patch-clamp recordings were obtained in voltage-clamp mode using a MultiClamp 700B amplifier (Molecular Devices) and pClamp (version 10.2) software. The patch pipette (3–5 MΩ resistance) was filled with a cesium methanesulfonate solution containing the following (in mM): 130 Cs-methanesulfonate, 10 CsCl, 4 NaCl, 1 $MgCl_2$, 5 MgATP, 5 EGTA, 10 HEPES, 5 GTP, 10 phosphocreatine, and 0.1 leupeptin. Electrode access resistances were <25 MΩ. Cells were held at −70 mV and spontaneous excitatory postsynaptic currents (sEPSCs) recorded for 3–5 min in the presence of picrotoxin (50 μM) to block $GABA_A$ receptor activation. Spontaneous inhibitory postsynaptic currents (sIPSCs) were recorded with the same internal solution used for EPSCs but holding the membrane at +10 mV to increase the driving force for Cl^- ions (reversal potential at −60 mV) and with the addition of the appropriate glutamate receptor antagonists 6-cyano-7-nitroquinoxaline-2,3-

dione (CNQX, 5 μM) and amino-5-phosphonovaleric acid (AP5, 50 μM). Postsynaptic currents were filtered at 1 kHz with Clampex 10.2 in gap-free mode. sEPSCs and sIPSCs were analyzed off-line with the automated detection protocol within the Mini Analysis program (Synaptosoft, version 6.0) and subsequently checked manually for accuracy. The threshold amplitudes for the detection of events were 5 pA for sEPSCs and 10 pA for sIPSCs. Event analyses were performed blind to genotype.

Ketogenic Diet (KD)

The chronic effects of the KD were examined in symptomatic R6/2 mice at two stages of disease progression, early symptomatic (~45 days) and fully symptomatic (>60 days). In this experiment one group of pregnant dams was fed a KD and another group received regular diet. Breeders for KD mice were acclimated to the diet one week prior to pairing. High-fat KD 5TJQ (Catalog # 1810844) was purchased from TestDiet (St. Louis, MO) and stored at 4°C until feeding. The formula contained no carbohydrates and the ratio protein:fat was ~1:5, which provides about 84% energy from fat and 16% energy from protein. Food was changed every 3–4 days. After weaning and genotyping (3–4 weeks of age), WT and R6/2 mice from dams fed a KD continued their pre-weaning regimen. Body weights were measured every week beginning at 4 weeks.

Behavioral Testing

Behavioral testing for R6/2 mice at 45 and 60 days of age was performed during the light phase of the light-dark cycle between 7:00 and 10:00 AM. Open field activity was assessed in a single 15-min session, with 15 data collection bins of 1 min each. Each mouse was placed individually in a square Plexiglas enclosure (40 cm X 40 cm) equipped with two photobeam sensor rings with a 32 X 32 array of infrared photocells for measuring horizontal and vertical movements (Coulbourn Instruments, Whitehall, PA). Movement was quantified automatically using TruScan software. Outcome measures included movement time, movement distance, velocity, and stereotypic movements. Stereotypic movements were defined by a series of coordinate changes less than ±0.999 beam spaces (in either the horizontal or vertical plane) and back to the starting point no more than 2 sec apart. Although stereotypic movements are used to measure repetitive behavior that does not contribute to large location changes, such movements cause beam breaks and thus contribute to overall distance. Thus, movement time and distance measures were obtained by subtracting stereotypic movements from the total movement time and total distance. After each session, the equipment was cleaned with an ammonium chloride disinfectant (Conflikt; Decon Labs, King of Prussia, PA) to remove residual odors.

Mice also were tested on a rotarod (Omnitech Electronics Inc., Columbus, OH) using a linear accelerating rotation paradigm (5–40 rpm over 10 min). Each session consisted of a single set of 5 trials with at least a 1 min break between each trial. The latency to fall for each mouse was calculated as the average of each 5-trial session.

Histology

At the end of behavioral testing, some mice fed the KD were deeply anesthetized with isoflurane and intracardially perfused with cold 4% paraformaldehyde (PFA) dissolved in

PBS. Brains were then removed and postfixed overnight in 4% PFA. Brains were cryoprotected for 2 days in 20% sucrose in PBS then 30% sucrose for 2 days and frozen on dry ice. Slices (30 μm thickness) spanning the striatum from bregma (1.18–0.38 mm) were mounted and stained with cresyl violet. Sections (n=6–7) 180 μm apart were used for volumetric analyses. Striatal and lateral ventricular area were traced manually in slices from both sides using ImageJ Software (National Institutes of Health, Bethesda, MD). Volumes were calculated by multiplying the sum of the areas by the section thickness and recorded in cubic millimeters. In these measurements the experimenter was blind to the genotype.

Gas chromatography/mass spectrometry

GC/MS was used to measure total plasma and brain cholesterol and BHB levels in WT and R6/2 mice (>60 days of age) consuming regular diet or the KD. Duplicate samples were prepared from each specimen and the data from the two results were averaged. Plasma samples (5 μL) were mixed with methanol (100 μL) after the addition of internal standards [5 μgms each of $^{13}C_3$-cholesterol (Sigma Aldrich) and $^{13}C_4$-BHB (Cambridge Isotope Laboratories) in 5 μL of methanol], and after 30 min at room temperature (rt) the samples were centrifuged (16,000 × g, 5 min) and the supernatants were transferred to GC injector vials and dried under a gentle stream of nitrogen. Each sample was then treated with N,O-bis(trimethylsilyl)trifluoroacetamide (50 μL) containing 10% (v/v) trimethylchlorosilane and incubated (60° C, 60 min). Aliquots (1 μL, equivalent to 2% of the original sample) were injected onto a bonded-phase non-polar fused silica capillary column (HP5-MS, phenyl/dimethylpolysiloxane 5/95, 30 m × 0.25 mm, 0.10 μm film thickness; injector port 250° C) and eluted (constant flow, 1 mL/min) with helium (min/°C; 0′/50, 3′/50, 30′/320, 35′/320). The end of the column (GC/MS transfer line at 250°C) was inserted into the EI source (180°C, 70 eV) of a quadrupole mass spectrometer (Agilent 5975 XL MSD) operating in the positive ion selected ion monitoring mode (m/z 233 and 237 for the M^+ ions from BHB-TMS and $^{13}C_4$-BHB-TMS, respectively at retention time 12 min; and m/z 458 and 461 for the M^+ ions from cholesterol-TMS and $^{13}C_3$-cholesterol-TMS, respectively, and m/z 368 and 371 for the $[M\text{-}HOSi(CH_3)_3]^+$ fragment ions from the same two compounds, at retention time 30 min). Standards were prepared with each batch of biological samples with the same amount of internal standards and a range of cholesterol and BHB concentrations (0, 1, 2, 3, and 5 μgm, in duplicate). The data from the standards were used to construct calibration curves (ordinate, ratio of cholesterol or BHB peak areas/corresponding internal standard peak areas; abscissa amount of either cholesterol or BHB in each sample). The amounts of cholesterol and BHB in each biological sample were calculated by interpolation from the calibration curves. The results from the two cholesterol data sets (the M^+ and $[M\text{-}HOSi(CH_3)_3]^+$ signals) were in close agreement and the average was calculated and reported. Brain tissue samples were processed in an identical manner using a 1 mL of methanol/2 mg of tissue with the same amounts of internal standards and homogenization was carried out with an ultrasonic cell disrupter.

Statistical Analyses

All values in figures and text are presented as mean±SE. Differences between group means were assessed with Student's *t*-test and, when comparing more than two groups, with appropriate ANOVAs (one- or two-way with one or two repeated measures) followed by

Bonferroni *post-hoc* tests. When ANOVAs were used, appropriate F and p values for group interactions are reported in the figure legends. Differences were considered statistically significant if $p<0.05$. SigmaStat 3.5 (Systat Software, San Jose, CA) was used to perform all statistical analyses.

Results

Effects of Cholesterol

Slices from symptomatic R6/2 animals (n=7, aged 70±2 days) and control littermates (n=5) were incubated for 1 h in either regular ACSF (control condition) or in water-soluble cholesterol (10 μM) complexed with MCD. In regular ACSF, membrane properties of MSNs (n=9) from R6/2 mice demonstrated a significant increase in input resistance compared with MSNs (n=7) from control littermates (Table 1). Although this difference persisted in slices incubated in cholesterol, the input resistance of MSNs in cholesterol-treated slices from R6/2s was lower than that of MSNs incubated in ACSF (p=0.032). In addition, the decay time constant of MSNs treated with cholesterol was longer than that of MSNs incubated in regular ACSF (p=0.046). Cell membrane capacitance was not different between groups.

After determining the effects of cholesterol on basic membrane properties we then examined its effects on synaptic activity. sEPSCs were recorded at a holding potential of −70 mV in the presence of the $GABA_A$ receptor blocker picrotoxin. Confirming previous data, the frequency of sEPSCs recorded in regular ACSF was reduced in MSNs (n=9) from R6/2 compared with MSNs (n=7) from controls (1.3±0.3 Hz and 3.7±1 Hz respectively, p=0.023). This difference persisted in slices incubated in cholesterol (1.1±0.2 Hz, n=11 R6/2 MSNs and 3.6±0.7 Hz, n=7 control MSNs, $p<0.001$), indicating that the frequency of sEPSCs is not altered by the presence of cholesterol. In contrast, the increase in the frequency of sIPSCs previously reported in R6/2 animals [29, 38] and also confirmed here (6.7±0.7 Hz, n=15 R6/2 cells and WT: 3.8±0.7 Hz, n=9 WT cells, t=−2.684, p=0.014, Student's *t*-test) was modified after incubation in cholesterol (Fig. 1A). While the overall IPSC frequency of R6/2 MSNs incubated in cholesterol was only marginally reduced compared with that of MSNs incubated in regular ACSF (5.6±0.9 Hz and 6.9±0.7 Hz, n=14 and n=15 respectively, p=0.36) (Fig. 1B inset), the frequency of medium- to large-amplitude events was reduced. An amplitude-frequency histogram indicated that the decrease was evident for events larger than 30 pA (Fig. 1B). Similarly, a cumulative amplitude histogram revealed a statistically significant leftward shift in R6/2 MSNs treated with cholesterol (Fig. 1C), while a cumulative inter-event interval (IEI) only showed a slight, non-significant rightward shift (Fig. 1D). Spontaneous IPSCs in MSNs from WT animals were not affected by cholesterol incubation (mean frequency 3.8±0.7 Hz, n=9 control and 2.9±0.4 Hz, n=7 cholesterol, p=0.3). In addition, we also tested the effects of MCD alone and at a concentration 0.6 mM it had no effects on the frequency of sIPSCs (7.8±1.2 Hz in ACSF, n=4 cells and 7.1±1.3 Hz in MCD, n=4 cells).

Effects of BHB

BHB is the main ketone body and can provide energy required for metabolic processes in the absence of glucose [12]. BHB, in conjunction with pyruvate, has been used to produce an

enriched form of ACSF (eACSF) [32]. The rationale for using eACSF is that in HD mice glucose utilization is impaired, which may lead to metabolic stress [8, 9]. The effects of eACSF on spontaneous synaptic activity were tested in 4 symptomatic R6/2 mice (aged 81±10 days). The average frequency of sIPSCs of MSNs (n=8) in control ACSF was 7.2±0.9 Hz. After switching to eACSF, the average frequency was significantly reduced (5±0.5 Hz, p=0.039) (Fig. 2A,B **inset**). An amplitude-frequency histogram showed that reduced frequency occurred across amplitude bins but was more pronounced for events greater than 40 pA (Fig. 2B). The cumulative amplitude histogram showed a significant leftward shift (Fig. 2C), while the cumulative IEI histogram showed a rightward shift after eACSF application (Fig. 2D). The difference in IEIs was statistically significant for events with 100–300 ms intervals.

Effects of the LXR agonist T0901317

LXRs are key regulators of cholesterol and glucose homeostasis. Oxysterols, such as 24-OHC, are the natural ligands for LXRs but a number of non-steroidal synthetic ligands have been created, among them T0901317, and it has been suggested they could renormalize neuronal synaptic function [39]. We tested the effects of T0901317 on sEPSCs and sIPSCs. Slices from WT (n=5, ages 70±1.7 days) or symptomatic R6/2 mice (n=7, aged 68.3±1 days) were incubated for 1 h in regular ACSF or in ACSF containing T0901317 (10 μM). In slices from R6/2 mice incubated in T0901317, the average frequency of sIPSCs from MSNs (3.8±0.6 Hz, n=15) was significantly reduced compared with that of MSNs incubated in regular ACSF (6.9±1.5, n=14, p=0.047) **inset**). An amplitude-frequency histogram demonstrated that the reduction in frequency occurred across amplitude bins, and the differences in the 10–20 and 20–30 pA bins were statistically significant (Fig. 3A). Similarly, there was a significant rightward shift in the IEI distribution in slices incubated in T0901317 (Fig. 3C). The cumulative amplitude distribution was not different after application of the agonist (Fig. 3B). Incubation of WT slices in T0901317 did not affect the average frequency of sIPSCs (4.1±0.7, n=10 in control conditions and 3.2±0.6, n=10 in T0901317, p=0.36). Interestingly, there was a slight increase in average frequency of sEPSCs in MSNs incubated in T0901317 (3.9±0.5 Hz, n=10) compared with MSNs incubated in regular ACSF (2.8±0.4 Hz, n=10) but the difference was not statistically significant (p=0.095). In R6/2 mice, T0901317 did not affect sEPSC frequency (0.82±0.14 Hz in control conditions, n=14 cells and 0.80±0.13 Hz in T0901317, n=16 cells).

Effects of Simvastatin

Simvastatin has been widely used to reduce cholesterol levels. Thus we used this drug to compare and contrast with the effects of cholesterol. Slices from WT (n=7, aged 69.1±2 days) or symptomatic R6/2 (n=10, aged 69.7±2 days) mice were incubated for 1 h in regular ACSF or in ACSF containing simvastatin (10 μM). In slices from R6/2 animals incubated in simvastatin, the average frequency of sIPSCs from MSNs (2.7±0.3 Hz, n=16) was significantly reduced compared with that of MSNs incubated in regular ACSF (4.5±0.4, n=18, p=0.002) (Fig. 3D **inset**). The amplitude-frequency histogram demonstrated that the reduction in frequency occurred across amplitude bins, and the differences in the 10–20 and 20–30 pA bins were statistically significant (Fig. 3D). Similarly, there was a significant rightward shift in the IEI distributions in slices incubated in simvastatin (Fig. 3F). The

cumulative amplitude distribution showed a slight leftward shift after agonist application that was significantly different for the 20 pA amplitude bin (Fig. 3E). Simvastatin did not affect sIPSC frequency in WT animals (3.12±0.47 Hz in control conditions, n=12 cells and 3.48±0.53 Hz in simvastatin, n=13 cells). In slices from R6/2 animals there was a slight increase in average sEPSCs in MSNs incubated in simvastatin (1.4±0.2 Hz, n=8) compared with MSNs incubated in regular ACSF (0.9±0.2 Hz, n=9) but the difference was not statistically significant (p=0.075). In contrast, incubation in simvastatin did not affect sEPSCs in slices from WT mice (2.8±0.5 Hz, n=8 in control conditions and 3.2±0.4 Hz, n=10 in simvastatin).

Effects of the KD

The KD has been proven beneficial in a number of neurological disorders including epilepsy [34, 35] and Alzheimer's disease [36] but the exact mechanisms remain unknown. For this experiment, we started feeding this diet to the breeders and then to the progeny from conception until sacrifice. The KD for a period up to 11 weeks in R6/2 mice was well-tolerated and did not appear to have any deleterious effects.

Body Weight—Confirming a previous study [40], we observed delayed weight loss in HD mice fed with the KD (Fig. 4A, **left graph**). After 7 weeks of age, R6/2 mice fed a regular diet (n=18) stopped gaining weight and by 8 weeks they started losing weight. In contrast, WT mice (n=21) continued gaining weight. R6/2 mice fed the KD (n=28) initially gained more weight than animals fed a regular diet. By 8 weeks they stopped gaining weight and by 9 weeks they slowly started losing weight. At this age, the weight of WT mice fed a regular diet and R6/2 mice fed the KD had very similar weights. WT animals fed the KD (n=16) continued gaining weight as they aged and by 9 weeks they were the heaviest among all groups. Percent weight changes in WT and R6/2 mice fed the regular or KD at 9 weeks of age, the last point examined, demonstrated significant differences between groups (Fig. 4A, **right graph**) except for the comparison between WT on the regular diet and R6/2 on the KD.

Behavior—A number of behavioral measures were examined in the four groups at two different stages of disease progression for R6/2 animals, early symptomatic (~45 d) and fully symptomatic (~60 d). At 45 days R6/2 mice (n=20 regular diet and n=25 KD) had a significantly reduced latency to fall on the accelerating rotarod compared to WTs (n=23 regular diet and n=14 KD) regardless of the diet. At 60 days the latency to fall was increased compared to 45 days in WT mice. In contrast, the latency to fall was further decreased in R6/2 mice (n=15 regular diet and n=20 KD) compared to WTs (n=15 regular diet and n=11 KD) regardless of the diet. The KD did not improve performance of R6/2 mice in the rotarod test (Fig. 4B). However, the KD rescued behaviors of 45d R6/2 mice in the open field. R6/2 mice fed the KD (n=33) moved significantly more, traveled farther, and faster compared with their R6/2 counterparts fed a regular diet (n=14) (Fig. 5A,B,C,D, **left panels**). Their behavior in the open field was similar to that of WT mice (n=15 regular diet and n=21 KD). In addition, the number of stereotypic movements, which are significantly higher in R6/2 compared with WT mice, was reduced in R6/2 mice fed the KD although the difference between R6/2 groups was not statistically significant (p=0.091) (Fig. 5E **left panel**). By 60

days the partial and transient improvement of these behaviors was diminished and only non-significant trends remained (Fig. 5A–E, **right panels**).

Electrophysiology—Mice in the four groups were sacrificed at ~50 days (3–5 mice per group) or ~70 days (4–8 mice per group) for slice electrophysiological recordings. Basic membrane properties of MSNs (cell membrane capacitance, input resistance and decay time constant) and spontaneous synaptic activity were assessed using whole-cell voltage clamp recordings. In early symptomatic animals, a significant increase in membrane input resistance of MSNs from R6/2 mice was observed regardless of the diet. Other basic membrane properties or the frequency of glutamatergic or GABAergic activity were not affected significantly (data not shown). Similarly, in fully symptomatic animals only mild, but non-significant trends were observed. Compared with R6/2 mice consuming a regular diet, in R6/2 fed the KD the input resistance of MSNs and the average frequency of spontaneous GABAergic currents were marginally reduced (Table 1 and Fig. 6A,B). Similarly, the reduction in sEPSC frequency was not significantly affected by the KD (Fig. 6C,D).

Histopathology—As the KD delayed weight loss in R6/2 mice, we also examined striatal and ventricle volumes in a subset of WT (n=4) and R6/2 (n=6) animals consuming the KD, expecting to see some rescue in R6/2 mice. Striatal volume was significantly (p=0.047) reduced in R6/2 (6.1±0.15 mm^3) compared with WT (6.9±0.36 mm^3) mice and the ventricle volume was significantly (p=0.005) increased in R6/2 (1.26±0.16 mm^3) compared with WT (0.46±0.07 mm^3) mice. Thus, despite delaying weight loss, the KD did not prevent brain atrophy in symptomatic R6/2 animals.

Cholesterol and BHB levels—GC/MS was used to measure cholesterol and BHB in plasma and brain from WT and R6/2 mice taking the regular diet or the KD. In line with previous reports [21, 41], plasma cholesterol levels were reduced in R6/2 compared with WT mice on a regular diet (t=2.358, p=0.029, Student's *t*-test). However, the comparison among the different groups did not yield a statistically significant interaction (Fig. 7A). Plasma BHB was not significantly changed by the KD in WT animals. However, BHB levels were significantly reduced in WT mice on the KD compared with R6/2 mice on a regular diet, as well as a trend for reduced BHB in R6/2 mice consuming the KD compared with the regular diet (Fig. 7B). Significant changes in free cholesterol content were found in brain tissue from R6/2 mice but were opposite to those occurring in plasma (Fig. 7C). A statistically significant elevation of brain cholesterol levels occurred in R6/2 compared with WT brains. Notably, the KD reduced cholesterol content and made it similar to that of WT mice under the KD (Fig. 7C). BHB was not significantly altered in WT or R6/2 animals regardless of the diet. Only the comparison between WT mice on the regular diet and R6/2 mice on the KD showed a statistically significant difference (Fig. 7D).

Discussion

These studies demonstrate that modulating lipid metabolism can produce a partial improvement of the behavioral and electrophysiological phenotype in the R6/2 mouse model of HD. Experiments *in vitro* demonstrated that acute application of cholesterol, ketone

bodies such as BHB, and LXR agonists clearly dampened the increase in sIPSC amplitude and/or frequency observed in R6/2 MSNs. Surprisingly, simvastatin also improved this synaptic phenotype. While cholesterol modulation readily affected sIPSC frequency, there was little or no effect on sEPSCs. Experiments *in vivo* demonstrated that the KD delayed weight loss and ameliorated some behavioral symptoms in the early stages. The KD however did not affect other phenotypic changes including rotarod performance, electrophysiological alterations, and brain atrophy.

While numerous studies have demonstrated early and long-lasting alterations in the cholesterol biosynthetic pathway in HD patients (however see [42]), and in genetic mouse models of HD including the R6/2 and YAC128 [43, 44], there has been controversy regarding cholesterol levels in the brain. Whereas some evidence points to dramatic downregulation of cholesterol in the brain [22, 44, 45], there also is evidence that, in spite of progressive reduction of brain cholesterol biosynthesis, steady-state levels of total cholesterol remain constant, suggesting compensatory mechanisms [21]. In support, a recent study reported that at least one precursor in the Bloch cholesterol synthetic pathway (desmosterol) is increased in R6/1 mice [31], thus supporting compensatory mechanisms to keep steady levels of cholesterol. Other studies have suggested that in HD cholesterol accumulates in the brain and this can become neurotoxic [46–49]. Such discrepancies could stem from the use of different HD models and methods of detection [14, 50, 51]. Alternatively, they could reflect different stages of disease progression [48] or that decreased sterol synthesis and accumulation of cholesterol in neuronal membranes represent two distinct mechanisms likely affecting neuronal survival in HD [52]. In agreement, it was recently shown that altered cholesterol homeostasis in HD results from decreased cholesterol synthesis and dysregulation of its clearance due deficient expression of CYP46A1, the rate limiting enzyme for cholesterol degradation [53]. Our GC/MS results suggest that, in mice consuming a regular diet, cholesterol levels in plasma are reduced in HD. However, in brain tissue cholesterol levels are increased, supporting that it may initially accumulate and trigger homeostatic mechanisms aimed at reducing *de novo* synthesis.

The present findings indicate that cholesterol and the ketone body BHB, when added to the ACSF solution, effectively reversed increases in sIPSC frequency and/or amplitude, in particular large-amplitude, activity-dependent synaptic events. The eACSF solution, containing BHB and pyruvate, has been used in slices from developing animals as it provides a number of nutrients that more closely mimic the energy sources used in early postnatal life [32, 54]. BHB also affects the functional state of neuronal networks in adult slices [55] and in itself can have neuroprotective and antiepileptic properties [56]. Pyruvate in the eACSF could also play a role as studies have shown neuroprotective effects of pyruvate [57]. Thus, at the present time we cannot distinguish if the effect is due to BHB or pyruvate acting as extra fuel for glucose compromised neurons or to additional effects. It has been shown for example that BHB blocks NLRP3 inflammasome-mediated inflammatory responses [58] and pyruvate is a potent antioxidant, augments glycogen stores, and also is a potent anti-inflammatory [57].

Cholesterol homeostasis in the brain is regulated by LXRs acting as cholesterol sensors, and protecting cells from cholesterol overload [33]. Synthetic oxysterol-mimetic drugs that

activate LXRs provide novel therapeutics for management of Alzheimer's disease and other neurological disorders characterized by altered tissue cholesterol homeostasis [59]. Members of nuclear receptor subfamily 1, which include LXRs, interact with Htt. Expansion of the polyglutamine tract in mHtt inhibits its binding to nuclear receptors and its ability to activate LXR transcription, suggesting that WT Htt could be involved in the regulation of cholesterol homeostasis [39]. In Htt-deficient zebrafish, T0901317 partially rescues the phenotype, providing evidence that activation of LXRs with appropriate agonists could renormalize neuronal synaptic function [39]. The present results indicate that this is at least partially true. However, some of the beneficial effects of LXR agonists also can be attributed to their ability to suppress neuroinflammation [60].

A surprising finding was that simvastatin, a drug typically used to reduce cholesterol, also improved the synaptic phenotype, casting doubt about the specificity of cholesterol effects. However, it is well known that simvastatin has pleiotropic effects besides lowering cholesterol levels. If, as some studies postulate [46], cholesterol is accumulated in HD cell membranes, simvastatin could enhance mobilization, redistribution, and/or efflux of accumulated cholesterol [61]. Simvastatin also increases membrane fluidity, has anti-inflammatory effects, and promotes BDNF production. This is important as we showed previously that BDNF reduces the increase in sIPSCs in R6/2 mice [29]. In addition, there is evidence that simvastatin can have neuroprotective effects in HD [47].

The KD delayed the occurrence of some peripheral symptoms of HD, including weight loss and some behavioral indices. The benefits of the KD have been extensively demonstrated in neurological disorders including epilepsy, Alzheimer's and Parkinson's diseases [34, 62]. The mechanisms are not well understood but could involve enhanced energy reserves that improve the ability of neurons to resist metabolic challenges [63], such as those associated with HD [62]. The KD also increases the production of BHB and while cholesterol and fatty acids do not appear to cross the BBB, ketones can enter the brain and serve as energy substrates [37]. Another hypothesis is that the KD affects kynurenic acid (KynA) production in the brain. KynA is a metabolite of tryptophan and has been used to block excitatory neurotransmission [64], including that mediated by N-methyl-D-aspartate (NMDA) glutamate receptors [65]. It was recently demonstrated *in vivo* that the KD produces large increases in BHB and also in KynA with anatomical specificity, as they occurred in hippocampus and striatum but not in cerebral cortex [66]. This is important as the KynA pathway is disrupted in HD and could be involved in the etiology of the disease [67].

There are only a handful of studies on the effects of different diets in HD models. Essential fatty acids (phospholipid components of cell membranes) given from conception prevented weight loss and behavioral deficits in R6/1 mice [68] and one study specifically using the KD in R6/2 mice reported some beneficial effects, including delayed weight loss, and no obvious deleterious effects [40]. Considering that in HD energy metabolism is significantly altered due to reduced gluconeogenesis in spite of increased demand, we expected that these alterations could be rescued in animals treated with a KD. Although weight loss and some behavioral symptoms were improved, the synaptic phenotype was practically unaffected. While acutely BHB ameliorated GABA synaptic alterations, in chronic conditions such as the KD, there was no improvement in spite of the fact that the KD produced slight, but not

statistically significant, increases of BHB levels in the brain. This could explain the lack of effects on sIPSCs as compared with acute administration of BHB and suggests that brain metabolism cannot rely permanently on energy derived from ketone metabolism.

Limitations

Although suggestive, the present results have important limitations. Because most drugs used in acute conditions have pleiotropic effects, it is difficult to determine which changes were due solely to effects on lipid metabolism. In addition, measurements of cholesterol after acute treatments in slices are indicated to better determine if the effects involve changes in cholesterol/ketone levels or also involve effects on neuroinflammation, which is prominent in mouse models of HD [69–71]. A previous study using filipin III staining showed that, in the case of statins or MCD, incubation of cell cultures effectively reduced free cholesterol levels [16]. Finally, different doses of cholesterol-modifying drugs should be tested, both *in vitro* and *in vivo*, to have a more complete picture of potential mechanisms.

Conclusions

Because of its widespread distribution [72], the repercussions of the Htt mutation are enormous and extend beyond the brain [8, 73]. Thus, therapeutic trials targeting only the brain regions where the most obvious pathology occurs are not likely to succeed. Only an integral treatment of body and brain alterations will alleviate the wide gamut of HD symptoms [74]. A step forward could be a combination therapy including a special diet and direct administration of cholesterol into the brain, e.g., by using modified cholesterol nanoparticles able to cross the BBB [75], or by stimulating cholesterol metabolism and efflux if, as some studies suggest, it accumulates in brain cell membranes [46, 53].

Acknowledgments

The authors would like to acknowledge Dr. Prasad R. Joshi, Krista Rudberg and Catherine Wang for their help with data acquisition and analysis during the early stages of this study. We also thank Dr. Vahri Beaumont, from CHDI Inc., for suggesting the use of LXR agonists in our studies. Donna Crandall helped with the illustrations. This work received support from USPHS grants NS081335 (CC) and NS41574 (MSL).

References

1. Vonsattel JP, DiFiglia M. Huntington disease. J Neuropathol Exp Neurol. 1998; 57:369–84. [PubMed: 9596408]
2. Rosas HD, Hevelone ND, Zaleta AK, Greve DN, Salat DH, Fischl B. Regional cortical thinning in preclinical Huntington disease and its relationship to cognition. Neurology. 2005; 65:745–7. [PubMed: 16157910]
3. Petersen A, Gil J, Maat-Schieman ML, Bjorkqvist M, Tanila H, Araujo IM, et al. Orexin loss in Huntington's disease. Hum Mol Genet. 2005; 14:39–47. [PubMed: 15525658]
4. Heinsen H, Rub U, Gangnus D, Jungkunz G, Bauer M, Ulmar G, et al. Nerve cell loss in the thalamic centromedian-parafascicular complex in patients with Huntington's disease. Acta Neuropathol. 1996; 91:161–8. [PubMed: 8787149]
5. Marder K, Zhao H, Eberly S, Tanner CM, Oakes D, Shoulson I. Dietary intake in adults at risk for Huntington disease: analysis of PHAROS research participants. Neurology. 2009; 73:385–92. [PubMed: 19652143]

6. Lalic NM, Maric J, Svetel M, Jotic A, Stefanova E, Lalic K, et al. Glucose homeostasis in Huntington disease: abnormalities in insulin sensitivity and early-phase insulin secretion. Arch Neurol. 2008; 65:476–80. [PubMed: 18413469]
7. Wilcox G. Insulin and insulin resistance. Clin Biochem Rev. 2005; 26:19–39. [PubMed: 16278749]
8. Bjorkqvist M, Fex M, Renstrom E, Wierup N, Petersen A, Gil J, et al. The R6/2 transgenic mouse model of Huntington's disease develops diabetes due to deficient beta- cell mass and exocytosis. Hum Mol Genet. 2005; 14:565–74. [PubMed: 15649949]
9. Hurlbert MS, Zhou W, Wasmeier C, Kaddis FG, Hutton JC, Freed CR. Mice transgenic for an expanded CAG repeat in the Huntington's disease gene develop diabetes. Diabetes. 1999; 48:649–51. [PubMed: 10078572]
10. Fain JN, Del Mar NA, Meade CA, Reiner A, Goldowitz D. Abnormalities in the functioning of adipocytes from R6/2 mice that are transgenic for the Huntington's disease mutation. Hum Mol Genet. 2001; 10:145–52. [PubMed: 11152662]
11. Hult S, Soylu R, Bjorklund T, Belgardt BF, Mauer J, Bruning JC, et al. Mutant huntingtin causes metabolic imbalance by disruption of hypothalamic neurocircuits. Cell Metab. 2011; 13:428–39. [PubMed: 21459327]
12. Cahill GF Jr, Veech RL. Ketoacids? Good medicine? Trans Am Clin Climatol Assoc. 2003; 114:149–61. discussion 62–3. [PubMed: 12813917]
13. Klosinski LP, Yao J, Yin F, Fonteh AN, Harrington MG, Christensen TA, et al. White Matter Lipids as a Ketogenic Fuel Supply in Aging Female Brain: Implications for Alzheimer's Disease. EBioMedicine. 2015; 2:1888–904. [PubMed: 26844268]
14. Valenza M, Cattaneo E. Emerging roles for cholesterol in Huntington's disease. Trends Neurosci. 2011; 34:474–86. [PubMed: 21774998]
15. Dietschy JM, Turley SD. Thematic review series: brain Lipids. Cholesterol metabolism in the central nervous system during early development and in the mature animal. J Lipid Res. 2004; 45:1375–97. [PubMed: 15254070]
16. Wasser CR, Ertunc M, Liu X, Kavalali ET. Cholesterol-dependent balance between evoked and spontaneous synaptic vesicle recycling. J Physiol. 2007; 579:413–29. [PubMed: 17170046]
17. Hering H, Lin CC, Sheng M. Lipid rafts in the maintenance of synapses, dendritic spines, and surface AMPA receptor stability. J Neurosci. 2003; 23:3262–71. [PubMed: 12716933]
18. Valencia A, Reeves PB, Sapp E, Li X, Alexander J, Kegel KB, et al. Mutant huntingtin and glycogen synthase kinase 3-beta accumulate in neuronal lipid rafts of a presymptomatic knock-in mouse model of Huntington's disease. J Neurosci Res. 2010; 88:179–90. [PubMed: 19642201]
19. Katsuno M, Adachi H, Sobue G. Getting a handle on Huntington's disease: the case for cholesterol. Nat Med. 2009; 15:253–4. [PubMed: 19265827]
20. Orth M, Bellosta S. Cholesterol: its regulation and role in central nervous system disorders. Cholesterol. 2012; 2012:292598. [PubMed: 23119149]
21. Valenza M, Leoni V, Tarditi A, Mariotti C, Bjorkhem I, Di Donato S, et al. Progressive dysfunction of the cholesterol biosynthesis pathway in the R6/2 mouse model of Huntington's disease. Neurobiol Dis. 2007; 28:133–42. [PubMed: 17702587]
22. Valenza M, Rigamonti D, Goffredo D, Zuccato C, Fenu S, Jamot L, et al. Dysfunction of the cholesterol biosynthetic pathway in Huntington's disease. J Neurosci. 2005; 25:9932–9. [PubMed: 16251441]
23. Cepeda C, Wu N, Andre VM, Cummings DM, Levine MS. The corticostriatal pathway in Huntington's disease. Prog Neurobiol. 2007; 81:253–71. [PubMed: 17169479]
24. Cepeda C, Hurst RS, Calvert CR, Hernandez-Echeagaray E, Nguyen OK, Jocoy E, et al. Transient and progressive electrophysiological alterations in the corticostriatal pathway in a mouse model of Huntington's disease. J Neurosci. 2003; 23:961–9. [PubMed: 12574425]
25. Klapstein GJ, Fisher RS, Zanjani H, Cepeda C, Jokel ES, Chesselet MF, et al. Electrophysiological and morphological changes in striatal spiny neurons in R6/2 Huntington's disease transgenic mice. J Neurophysiol. 2001; 86:2667–77. [PubMed: 11731527]
26. Cummings DM, Milnerwood AJ, Dallerac GM, Waights V, Brown JY, Vatsavayai SC, et al. Aberrant cortical synaptic plasticity and dopaminergic dysfunction in a mouse model of Huntington's disease. Hum Mol Genet. 2006; 15:2856–68. [PubMed: 16905556]

27. Cummings DM, Cepeda C, Levine MS. Alterations in striatal synaptic transmission are consistent across genetic mouse models of Huntington's disease. ASN Neuro. 2010; 2:e00036. [PubMed: 20585470]
28. Andre VM, Cepeda C, Fisher YE, Huynh M, Bardakjian N, Singh S, et al. Differential electrophysiological changes in striatal output neurons in Huntington's disease. J Neurosci. 2011; 31:1170–82. [PubMed: 21273402]
29. Cepeda C, Starling AJ, Wu N, Nguyen OK, Uzgil B, Soda T, et al. Increased GABAergic function in mouse models of Huntington's disease: reversal by BDNF. J Neurosci Res. 2004; 78:855–67. [PubMed: 15505789]
30. Gil JM, Rego AC. The R6 lines of transgenic mice: a model for screening new therapies for Huntington's disease. Brain Res Rev. 2009; 59:410–31. [PubMed: 19118572]
31. Kreilaus F, Spiro AS, Hannan AJ, Garner B, Jenner AM. Brain Cholesterol Synthesis and Metabolism is Progressively Disturbed in the R6/1 Mouse Model of Huntington's Disease: A Targeted GC-MS/MS Sterol Analysis. J Huntingtons Dis. 2015; 4:305–18. [PubMed: 26639223]
32. Holmgren CD, Mukhtarov M, Malkov AE, Popova IY, Bregestovski P, Zilberter Y. Energy substrate availability as a determinant of neuronal resting potential, GABA signaling and spontaneous network activity in the neonatal cortex in vitro. J Neurochem. 2010; 112:900–12. [PubMed: 19943846]
33. Zhao C, Dahlman-Wright K. Liver X receptor in cholesterol metabolism. J Endocrinol. 2010; 204:233–40. [PubMed: 19837721]
34. Rho JM, Stafstrom CE. The ketogenic diet: what has science taught us? Epilepsy Res. 2012; 100:210–7. [PubMed: 21856126]
35. Felton EA, Cervenka MC. Dietary therapy is the best option for refractory nonsurgical epilepsy. Epilepsia. 2015; 56:1325–9. [PubMed: 26198999]
36. Stafstrom CE, Rho JM. The ketogenic diet as a treatment paradigm for diverse neurological disorders. Front Pharmacol. 2012; 3:59. [PubMed: 22509165]
37. Nehlig A. Brain uptake and metabolism of ketone bodies in animal models. Prostaglandins Leukot Essent Fatty Acids. 2004; 70:265–75. [PubMed: 14769485]
38. Cepeda C, Galvan L, Holley SM, Rao SP, Andre VM, Botelho EP, et al. Multiple sources of striatal inhibition are differentially affected in Huntington's disease mouse models. J Neurosci. 2013; 33:7393–406. [PubMed: 23616545]
39. Futter M, Diekmann H, Schoenmakers E, Sadiq O, Chatterjee K, Rubinsztein DC. Wild- type but not mutant huntingtin modulates the transcriptional activity of liver X receptors. J Med Genet. 2009; 46:438–46. [PubMed: 19451134]
40. Ruskin DN, Ross JL, Kawamura M Jr, Ruiz TL, Geiger JD, Masino SA. A ketogenic diet delays weight loss and does not impair working memory or motor function in the R6/2 1J mouse model of Huntington's disease. Physiol Behav. 2011; 103:501–7. [PubMed: 21501628]
41. Leoni V, Caccia C. The impairment of cholesterol metabolism in Huntington disease. Biochim Biophys Acta. 2015; 1851:1095–105. [PubMed: 25596342]
42. Nambron R, Silajdzic E, Kalliolia E, Ottolenghi C, Hindmarsh P, Hill NR, et al. A Metabolic Study of Huntington's Disease. PLoS One. 2016; 11:e0146480. [PubMed: 26744893]
43. Valenza M, Cattaneo E. Cholesterol dysfunction in neurodegenerative diseases: is Huntington's disease in the list? Prog Neurobiol. 2006; 80:165–76. [PubMed: 17067733]
44. Valenza M, Leoni V, Karasinska JM, Petricca L, Fan J, Carroll J, et al. Cholesterol defect is marked across multiple rodent models of Huntington's disease and is manifest in astrocytes. J Neurosci. 2010; 30:10844–50. [PubMed: 20702713]
45. Valenza M, Marullo M, Di Paolo E, Cesana E, Zuccato C, Biella G, et al. Disruption of astrocyte-neuron cholesterol cross talk affects neuronal function in Huntington's disease. Cell Death Differ. 2015; 22:690–702. [PubMed: 25301063]
46. Trushina E, Singh RD, Dyer RB, Cao S, Shah VH, Parton RG, et al. Mutant huntingtin inhibits clathrin-independent endocytosis and causes accumulation of cholesterol in vitro and in vivo. Hum Mol Genet. 2006; 15:3578–91. [PubMed: 17142251]

47. del Toro D, Xifro X, Pol A, Humbert S, Saudou F, Canals JM, et al. Altered cholesterol homeostasis contributes to enhanced excitotoxicity in Huntington's disease. J Neurochem. 2010; 115:153–67. [PubMed: 20663016]
48. Luthi-Carter R, Taylor DM, Pallos J, Lambert E, Amore A, Parker A, et al. SIRT2 inhibition achieves neuroprotection by decreasing sterol biosynthesis. Proc Natl Acad Sci U S A. 2010; 107:7927–32. [PubMed: 20378838]
49. Taylor DM, Balabadra U, Xiang Z, Woodman B, Meade S, Amore A, et al. A brain- permeable small molecule reduces neuronal cholesterol by inhibiting activity of sirtuin 2 deacetylase. ACS Chem Biol. 2011; 6:540–6. [PubMed: 21370928]
50. Valenza M, Cattaneo E. Neuroprotection and brain cholesterol biosynthesis in Huntington's disease. Proc Natl Acad Sci U S A. 2010; 107:E143. author reply 4. [PubMed: 20807740]
51. Marullo M, Valenza M, Leoni V, Caccia C, Scarlatti C, De Mario A, et al. Pitfalls in the detection of cholesterol in Huntington's disease models. PLoS Curr. 2012; 4:e505886, e9a1968.
52. Karasinska JM, Hayden MR. Cholesterol metabolism in Huntington disease. Nat Rev Neurol. 2011; 7:561–72. [PubMed: 21894212]
53. Boussicault L, Alves S, Lamaziere A, Planques A, Heck N, Moumne L, et al. CYP46A1, the rate-limiting enzyme for cholesterol degradation, is neuroprotective in Huntington's disease. Brain. 2016; 139:953–70. [PubMed: 26912634]
54. Rheims S, Holmgren CD, Chazal G, Mulder J, Harkany T, Zilberter T, et al. GABA action in immature neocortical neurons directly depends on the availability of ketone bodies. J Neurochem. 2009; 110:1330–8. [PubMed: 19558450]
55. Ivanov A, Zilberter Y. Critical state of energy metabolism in brain slices: the principal role of oxygen delivery and energy substrates in shaping neuronal activity. Front Neuroenergetics. 2011; 3:9. [PubMed: 22232599]
56. Ramirez C, Tercero I, Pineda A, Burgos JS. Simvastatin is the statin that most efficiently protects against kainate-induced excitotoxicity and memory impairment. J Alzheimers Dis. 2011; 24:161–74. [PubMed: 21224519]
57. Zilberter Y, Gubkina O, Ivanov AI. A unique array of neuroprotective effects of pyruvate in neuropathology. Front Neurosci. 2015; 9:17. [PubMed: 25741230]
58. Youm YH, Nguyen KY, Grant RW, Goldberg EL, Bodogai M, Kim D, et al. The ketone metabolite beta-hydroxybutyrate blocks NLRP3 inflammasome-mediated inflammatory disease. Nat Med. 2015; 21:263–9. [PubMed: 25686106]
59. Cao G, Bales KR, DeMattos RB, Paul SM. Liver X receptor-mediated gene regulation and cholesterol homeostasis in brain: relevance to Alzheimer's disease therapeutics. Curr Alzheimer Res. 2007; 4:179–84. [PubMed: 17430244]
60. Zelcer N, Khanlou N, Clare R, Jiang Q, Reed-Geaghan EG, Landreth GE, et al. Attenuation of neuroinflammation and Alzheimer's disease pathology by liver × receptors. Proc Natl Acad Sci U S A. 2007; 104:10601–6. [PubMed: 17563384]
61. Burns MP, Igbavboa U, Wang L, Wood WG, Duff K. Cholesterol distribution, not total levels, correlate with altered amyloid precursor protein processing in statin-treated mice. Neuromolecular Med. 2006; 8:319–28. [PubMed: 16775383]
62. Gasior M, Rogawski MA, Hartman AL. Neuroprotective and disease-modifying effects of the ketogenic diet. Behav Pharmacol. 2006; 17:431–9. [PubMed: 16940764]
63. Bough K. Energy metabolism as part of the anticonvulsant mechanism of the ketogenic diet. Epilepsia. 2008; 49(Suppl 8):91–3. [PubMed: 19049599]
64. Birch PJ, Grossman CJ, Hayes AG. Kynurenate and FG9041 have both competitive and non-competitive antagonist actions at excitatory amino acid receptors. Eur J Pharmacol. 1988; 151:313–5. [PubMed: 2901972]
65. Ganong AH, Cotman CW. Kynurenic acid and quinolinic acid act at N-methyl-D- aspartate receptors in the rat hippocampus. J Pharmacol Exp Ther. 1986; 236:293–9. [PubMed: 2867215]
66. Zarnowski T, Choragiewicz T, Tulidowicz-Bielak M, Thaler S, Rejdak R, Zarnowski I, et al. Ketogenic diet increases concentrations of kynurenic acid in discrete brain structures of young and adult rats. J Neural Transm (Vienna). 2012; 119:679–84. [PubMed: 22200857]

67. Guidetti P, Luthi-Carter RE, Augood SJ, Schwarcz R. Neostriatal and cortical quinolinate levels are increased in early grade Huntington's disease. Neurobiol Dis. 2004; 17:455–61. [PubMed: 15571981]

68. Clifford JJ, Drago J, Natoli AL, Wong JY, Kinsella A, Waddington JL, et al. Essential fatty acids given from conception prevent topographies of motor deficit in a transgenic model of Huntington's disease. Neuroscience. 2002; 109:81–8. [PubMed: 11784701]

69. Chang KH, Wu YR, Chen YC, Chen CM. Plasma inflammatory biomarkers for Huntington's disease patients and mouse model. Brain Behav Immun. 2015; 44:121–7. [PubMed: 25266150]

70. Soulet D, Cicchetti F. The role of immunity in Huntington's disease. Mol Psychiatry. 2011; 16:889–902. [PubMed: 21519341]

71. Sapp E, Kegel KB, Aronin N, Hashikawa T, Uchiyama Y, Tohyama K, et al. Early and progressive accumulation of reactive microglia in the Huntington disease brain. J Neuropathol Exp Neurol. 2001; 60:161–72. [PubMed: 11273004]

72. Li SH, Schilling G, Young WS 3rd, Li XJ, Margolis RL, Stine OC, et al. Huntington's disease gene (IT15) is widely expressed in human and rat tissues. Neuron. 1993; 11:985–93. [PubMed: 8240819]

73. Strand AD, Aragaki AK, Shaw D, Bird T, Holton J, Turner C, et al. Gene expression in Huntington's disease skeletal muscle: a potential biomarker. Hum Mol Genet. 2005; 14:1863–76. [PubMed: 15888475]

74. Martin B, Golden E, Keselman A, Stone M, Mattson MP, Egan JM, et al. Therapeutic perspectives for the treatment of Huntington's disease: treating the whole body. Histol Histopathol. 2008; 23:237–50. [PubMed: 17999380]

75. Valenza M, Chen JY, Di Paolo E, Ruozi B, Belletti D, Ferrari Bardile C, et al. Cholesterol-loaded nanoparticles ameliorate synaptic and cognitive function in Huntington's disease mice. EMBO Mol Med. 2015; 7:1547–64. [PubMed: 26589247]

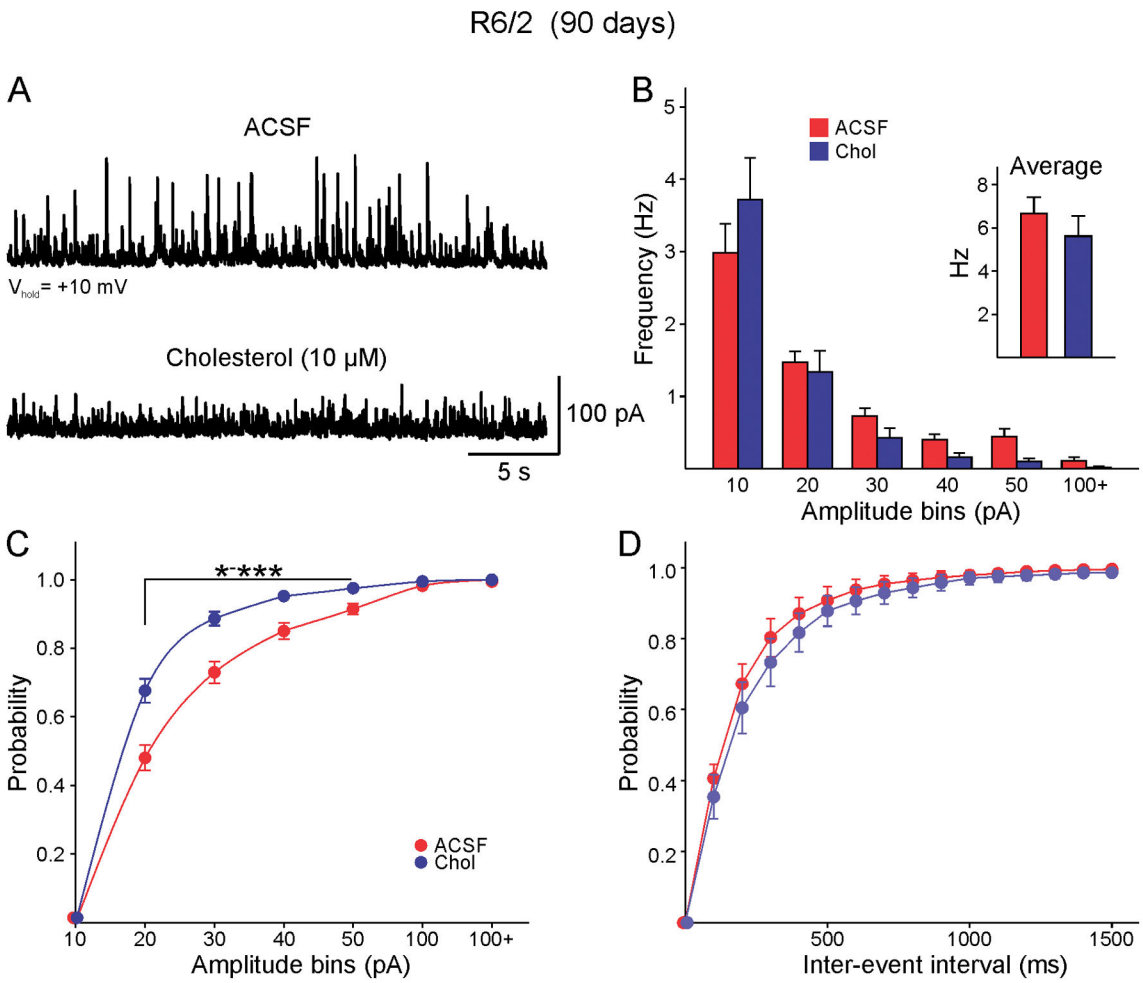

Fig. 1.

A. sIPSCs were recorded at a holding potential of +10mV from visually identified MSNs in the dorsal striatum from symptomatic R6/2 mice (>70 days of age). In regular ACSF cells displayed high frequency, large amplitude sIPSCs. Incubation with cholesterol resulted in a significant reduction of large amplitude currents. **B.** The average frequency of sIPSC was practically unchanged by incubation in cholesterol (inset). There was a trend towards reduced medium- and large-amplitude synaptic events (amplitudes larger than 30 pA). **C.** In agreement, the cumulative amplitude histogram demonstrated a significant leftward shift indicating a decrease in large amplitude events or proportionately more low-amplitude events [two-way RM ANOVA, $F(6,150)=13.782$, $p<0.001$]. Asterisks indicate bins with statistically significant differences after Bonferroni post-hoc test. In this and subsequent figures * $p<0.05$, ** $p<0.01$ and *** $p<0.001$. **D.** The cumulative inter-event interval (IEI) probability distribution did not show a significant difference.

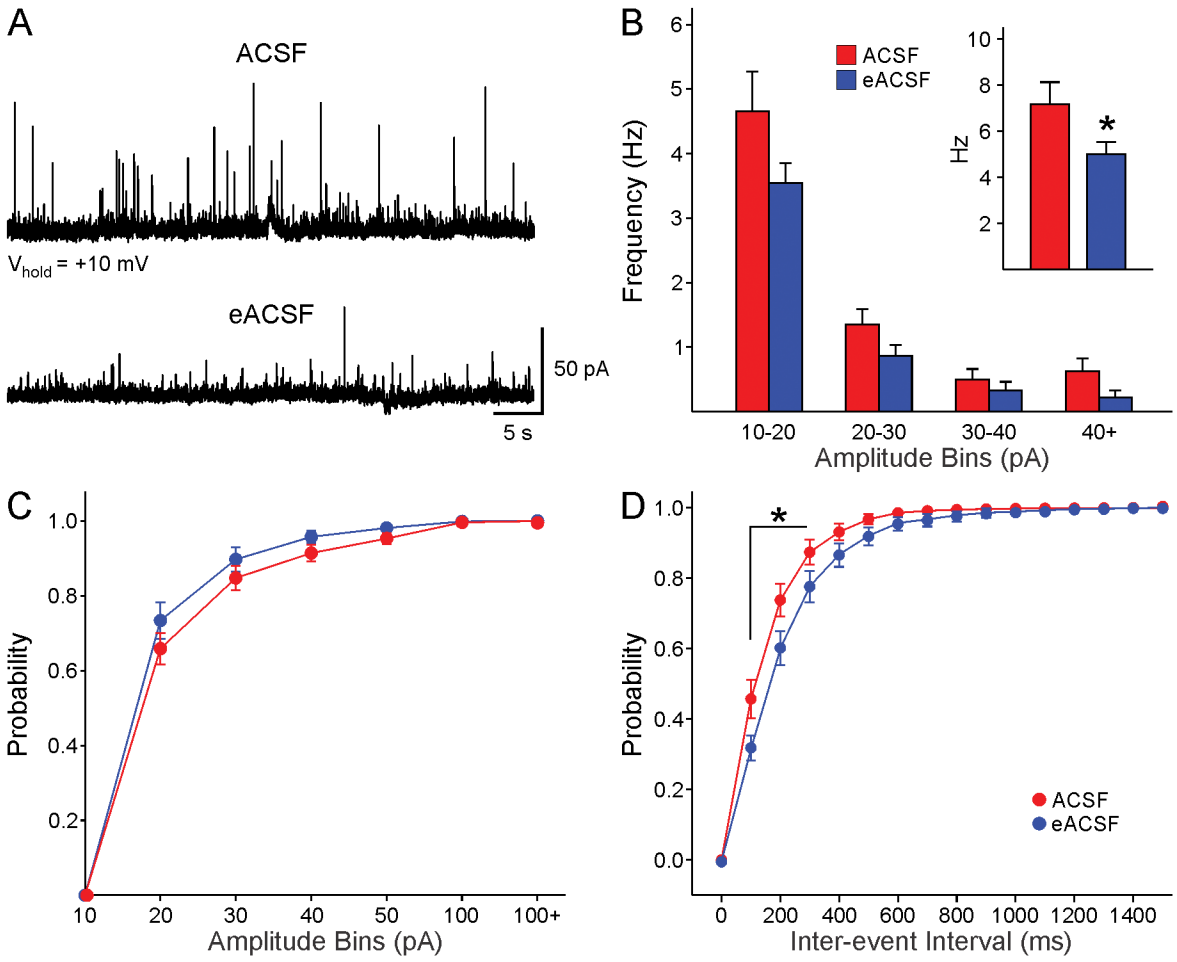

Fig. 2.

A. After recording basal sIPSCs, the external solution was changed to eACSF for 20 min. Traces show the effects of eACSF on sIPSCs in a MSN from a 70 day-old R6/2 mouse. **B.** The average frequency of events was reduced (Student's *t*-test, t=2.19, p=0.049). **C.** The cumulative amplitude distribution showed a small, non-significant leftward shift after eACSF, indicating only a trend for reduced number of large-amplitude events. **D.** The cumulative IEI probability distribution showed a rightward shift, indicating reductions in frequency after eACSF [two-way RM ANOVA, F(150,150)=3.669, p<0.001].

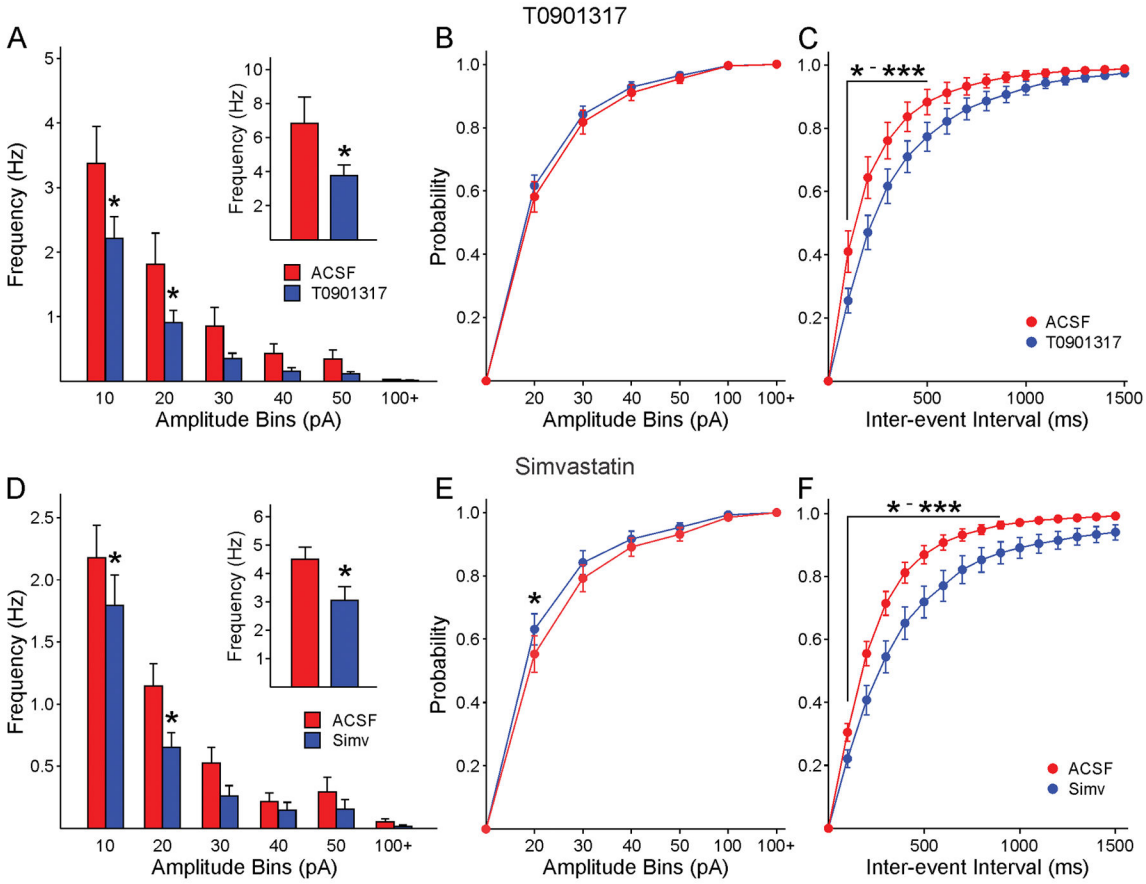

Fig. 3.

A. Incubation in T0901317 reduced the average frequency of IPSCs (inset). The amplitude-frequency histogram showed that the reduction occurred across amplitude bins [two-way RM ANOVA, F(5,135)=2.822, p=0.019]. **B.** The cumulative amplitude histogram showed no change after T0901317 [two-way RM ANOVA, F(6,162)=0.339, p=0.916]. **C.** The cumulative IEI histogram showed a significant rightward shift after T0901317 indicating a reduced frequency of synaptic events [two-way RM ANOVA, F=(15,405)=3.547, p<0.001]. **D.** Similar to the effects of the LXR agonist, incubation in Simvastatin reduced the average frequency of IPSCs (inset, Student's *t*-test, t=2.312, p=0.027). The amplitude-frequency histogram showed that the reduction occurred across amplitude bins [two-way RM ANOVA, F(5,165), p=0.365 (*post hoc* tests show p=0.045 for the 10 pA bin and p=0.010 for the 20 pA bin)]. **E.** Only a sight leftward shift in the cumulative amplitude distribution occurred after T0901317. **F.** The cumulative IEI histogram showed a significant rightward shift after Simvastatin indicating a reduced frequency of synaptic events [two-way RM ANOVA, F(15,495)=5.001, p<0.001].

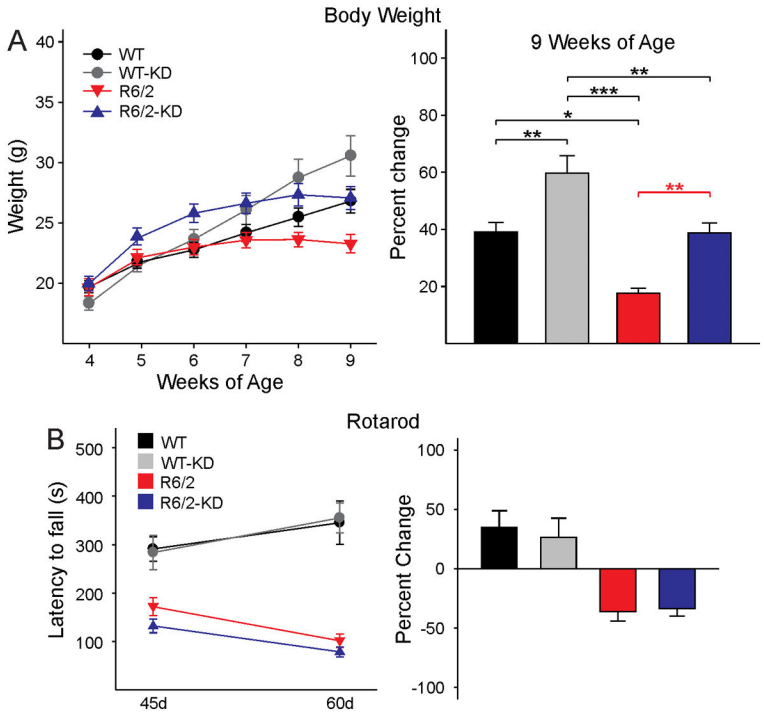

Fig. 4.

A. Effects of the KD on weight loss. Graph on the left shows absolute weight changes from 4–9 weeks of age in WT and R6/2 mice receiving regular chow or the KD. All animals gained weight from 4–6 weeks of age. By 7 weeks R6/2 mice on regular diet started losing weight while their WT littermates continued gaining weight. In contrast, R6/2 mice on the KD started losing weight after 8 weeks and the loss was less pronounced than in R6/2 mice fed regular chow. Graph on the right shows percent weight changes in WT and R6/2 mice fed the regular or KD at 9 weeks of age. There was a significant interaction among groups (one-way ANOVA, $F(3,67)=13.366$, $p<0.001$). Importantly, the weights from WT mice fed a regular diet were equivalent to those of R6/2 mice fed the KD. At this age the WT animals fed the KD were the heaviest. **B.** Performance on the rotarod improved similarly from 45 to 60 days in WT mice regardless of the diet. In contrast, the performance deteriorated similarly in R6/2 mice regardless of the diet [two-way RM ANOVA, $F(3,53)=8.384$, $p<0.001$].

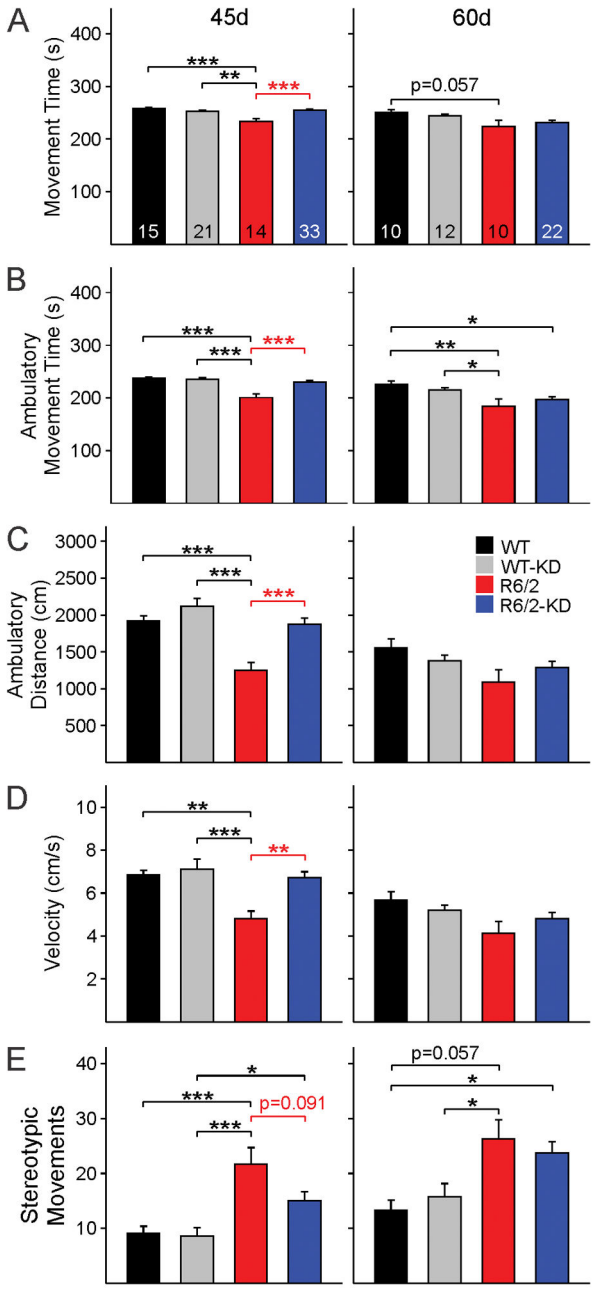

Fig. 5.

Open field behavior was tested at 45 and 60 days in WT and R6/2 mice fed a regular diet or the KD. At 45 days R6/2 mice on the KD performed as well as WT mice and, compared with R6/2 animals fed regular diet, showed significant improvements in total movement time **(A)**, ambulation time **(B)**, distance **(C)** and velocity **(D)**. There was a trend for reduced number of stereotypies but the difference did not reach statistical significance **(E).** Significant differences between R6/2 mice fed a regular diet and the KD are indicated by red asterisks. [One-way ANOVA for all panels, group interactions are as follows: **(A)** $F(3,79)=8.468$, $p<0.001$, **(B)** $F(3,79)=14.608$, $p<0.001$, **(C)** $F(3,79)=10.598$, $p<0.001$, **(D)**

F(3,79)=6.251, p<0.001, **(E)** F(3,79)=8.537, p<0.001]. At 60 days, behavioral differences between WT and R6/2 mice persisted [**(A)** F(3,53)=3.380, p=0.025, **(B)** F(3,53)=5.508, p=0.002, **(C)** F(3,53)=2.356, p=0.082, **(D)** F(3,53)=2.453, p=0.074, **(E)** F(3,53)=5.396, p=0.003]. However, the behavioral improvement in R6/2 mice on the KD was no longer present.

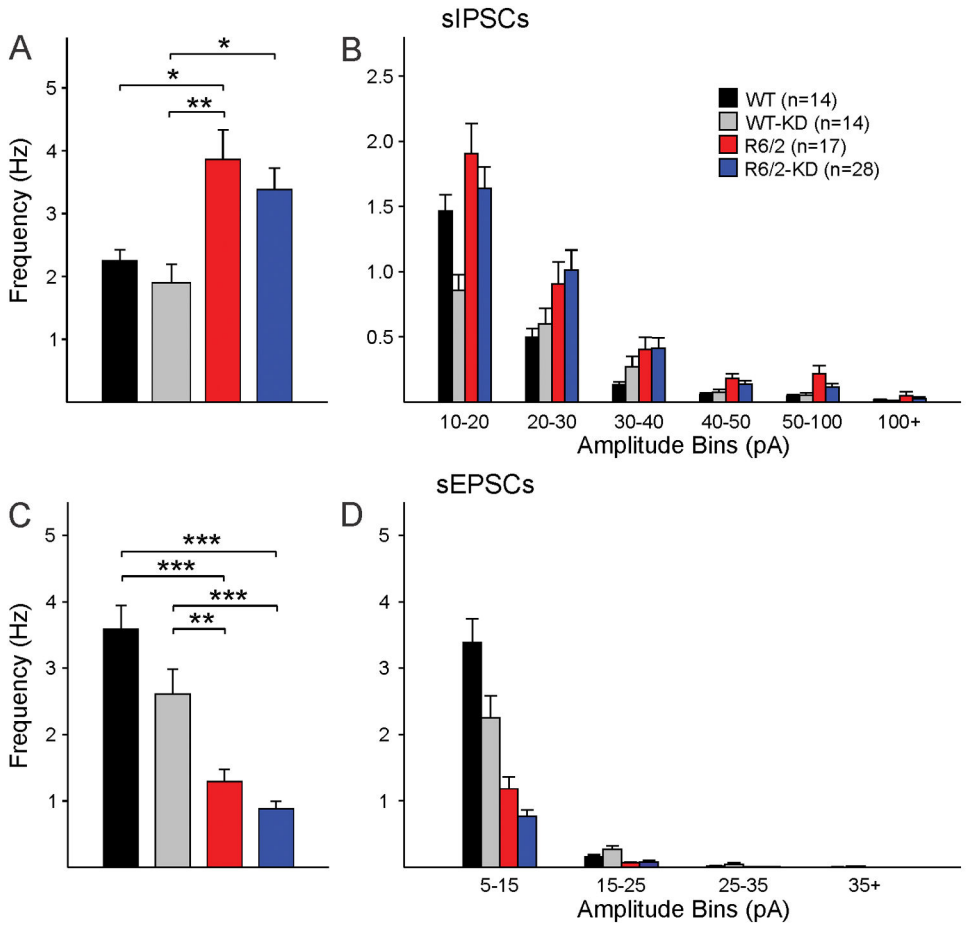

Fig. 6.

Effects of the KD on synaptic activity. As demonstrated previously, MSNs from R6/2 animals have increased frequency of sIPSCs [one-way ANOVA $F(3,69)=5.665$, $p=0.002$] **(A, B)** and reduced frequency of sEPSCs [one-way ANOVA $F(3,69)=28.223$, $p<0.001$] **(C, D)**. The KD did not improve this synaptic phenotype. Numbers in parentheses indicate the number of cells recorded.

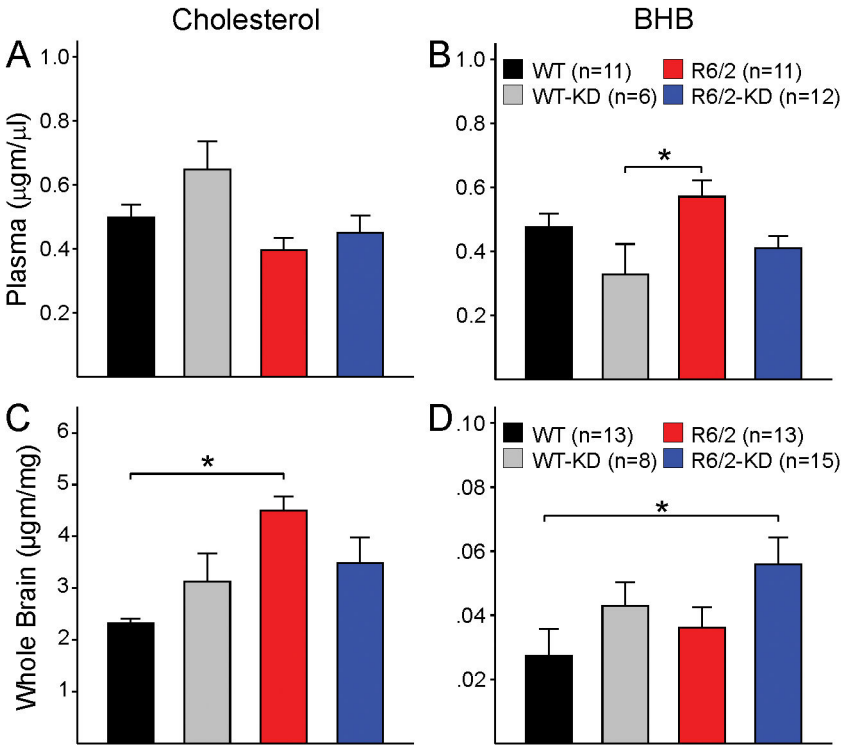

Fig. 7.

Plasma and brain cholesterol levels were determined using GC/MS in animals taking the regular or the KD. **(A)** Group comparisons showed no changes in plasma cholesterol levels across genotype and treatment groups [one-way ANOVA on ranks, H(3)=5.727, p=0.126]. **(B)** Plasma BHB levels were significantly reduced in WT mice on the KD compared with R6/2 mice on a regular diet [one-way ANOVA, F(3,35)=3.424, p=0.028] **(C)** There was a statistically significant increase in brain cholesterol levels in R6/2 compared with WT mice on a regular diet. Importantly, the difference was no longer present in R6/2 compared with WT animals on the KD. This was due to a non-significant increase of cholesterol levels in WTs and a significant reduction in cholesterol levels in R6/2 mice on the KD compared with those on a regular diet [one-way ANOVA on ranks, H(3)=13.026, p=0.005]. **(D)** Brain BHB levels were not different between WT and R6/2 mice on a regular diet but there was a significant increase in R6/2 mice on the KD compared with WT mice on a regular diet [one-way ANOVA on ranks, H(3)=8.247, p=0.041].

Table 1

Basic Membrane Properties of MSNs in regular ACSF and in ACSF Supplemented with Cholesterol

	Cap (pF)	Ri (MΩ)	Tau (ms)
WT Regular ACSF (n=11)	74.4±6.4	49.0±5.8	1.8±0.2
R6/2 Regular ACSF (n=13)	67.5±4.3	**145.0±20**	**1.5±0.1**
WT ACSF+Cholesterol (n=9)	62.3±6.0	37.7±3.3	2.0±0.2
R6/2 ACSF+ Cholesterol (n=14)	63.8±3.9	**98.4±9.9** *	**1.8±0.1** *

* For the sake of simplicity only statistically significant differences between ACSF and cholesterol treatment are indicated (in bold).

Table 2

Basic Membrane Properties of MSNs in Mice Fed a Regular Diet or the KD

	Cap (pF)	Ri (MΩ)	Tau (ms)
WT Regular Diet (n=14)	59.5±4.4	**44.5±6.5**	2.0±0.1
R6/2 Regular Diet (n=17)	62.6±3.4	**152.5±20.1** *	1.7±0.1
WT Ketogenic Diet (n=14)	71.9±4.3	**64.9±17.6**	**1.9±0.1**
R6/2 Ketogenic Diet (n=28)	64.3±3.0	**127.1±10.9** *	**1.6±0.1** *

* Asterisks indicate statistically significant differences between WT and R6/2 mice ages >60 days